Communications on Applied Electronics (CAE) – ISSN : 2394-4714
Foundation of Computer Science FCS, New York, USA
International Conference on Communication Technology (ICCT 2015) – www.caeaccess.org

# Artificial Neural Network Model for Suspended Shorted $90^0$ Sectoral Microstrip Antennas

Amit A. Deshmukh
Professor and Head, EXTC, DJSCOE, Vile-Parle (W), Mumbai, India

Shivali D. Kulkarni
ELEX, DJSCOE, Vile-Parle (W), Mumbai, India

Venkata A. P. C.
EXTC, DJSCOE, Vile-Parle (W), Mumbai, India

## ABSTRACT
The simplest way to realize broadband microstrip antenna is by selecting thicker air substrate for the radiating patch. The compact circular microstrip antenna is realized by placing the shorting plate/post along the zero field line at fundamental $TM_{11}$ mode and by using only half of the shorted patch. To increase the bandwidth of compact shorted microstrip antenna, thicker air substrate is used. While designing shorted circular microstrip antenna, frequency formulations used in for conventional circular microstrip antenna on thinner substrate, gives closer approximation. However design formulations to realize shorted compact circular microstrip antenna on thicker substrate over wide range of frequencies are not available. In this paper, an artificial neural network model to predict the shorted circular patch radius in shorted $90^0$ Sectoral microstrip antenna for varying frequencies and substrate thickness is proposed. The frequency calculated using the predicted shorted patch radius closely agrees with the simulated and measured shorted patch frequency.

## Keywords
Circular microstrip antenna, Compact microstrip antenna, Shorted $90^0$ Sectoral antenna, Artificial Neural Network model, Supervised Network, Back Propagation Algorithm

## 1. INTRODUCTION
By fabricating the radiating patch on lower dielectric constant thicker substrate, broadband microstrip antenna (MSA) has been realized [1 – 4]. In the available literature, radiating patch is suspended above the ground plane using air as the substrate. The air has dielectric constant of unity and the loss tangent of zero. Therefore use of air substrate helps in reducing the quality factor of the cavity below the patch thereby realizing larger BW. In MSAs, regular shapes for radiating patch like, rectangular, circular, equilateral triangular, etc are used. The resonance frequency formulation for these regular shapes on thinner substrates ($h \leq 0.03\lambda_0$), is available [1 – 4]. It is reported that radiation from the MSA is due to the fringing fields present towards patch periphery [1 – 4]. This fringing field changes the effective dimension of the patch and therefore extension in patch length along its periphery needs to be accounted while calculating patch resonance frequency. The equations for fringing field extension are available for thinner substrate for regular shaped MSAs.

The circular MSA (CMSA) and rectangular MSA are more commonly used MSAs since they shows radiation pattern with lower cross polar levels. Amongst the two when harmonic rejection is needed, CMSA are preferred as its fundamental and higher order mode resonance frequencies are governed by the ratios of $n^{th}$ root of $m^{th}$ order Bessel function of second type [1 – 4]. The compact CMSA is obtained by placing the shorting plate/post along the zero field line at $TM_{11}$ mode to yield shorted semi-circular MSA [1 – 4]. The compact shorted $90^0$ Sectoral MSA is obtained by using symmetry of shorted semi-circular MSA across the feed point axis and by using only half of the patch size [1 – 4]. The shorted $90^0$ Sectoral MSA gives nearly 75% reductions in patch size as compared to CMSA with nearly the same resonance frequency and % BW. The resonance frequency of shorted $90^0$ Sectoral MSA calculated by using resonance frequency equation for CMSA gives accurate results for substrate thickness less than 0.02 to $0.03\lambda_0$. However it gives larger error for higher substrate thickness. The larger error results due to error in calculation of edge extension length in shorted patches as the closed form expressions for the same are not available. The artificial neural network (ANN) model has been widely used to analyze MSAs [5 – 9]. However in the reported literature, ANN model for the MSA over wide range of frequencies and substrate thickness is not reported [5 – 9]. The ANN models to calculate the shorted patch dimension and edge extension length in terms of substrate thickness for shorted rectangular MSA as well as patch dimensions for rectangular MSA, are reported [10, 11]. They give patch dimensions for substrate thickness in the range of 0.03 to $0.1\lambda_0$ and over wide frequency range (600 to 6000 MHz). In this paper, an ANN model for predicting the radius of shorted $90^0$ Sectoral patch and the edge extension length in terms of substrate thickness over 800 to 6000 MHz frequency range and for air substrate having thickness in the range of $0.04\lambda_0$ to $0.1\lambda_0$ is proposed. The resonance frequency of shorted $90^0$ Sectoral MSA calculated using ANN model shows closer agreement with simulated and measured results. Thus the proposed model will be helpful to design shorted $90^0$ Sectoral MSA at any frequency on thicker air substrate. In the proposed work, first the training data set is generated using IE3D software using finite ground plane [12]. This was further used to develop ANN model. To generate the measured data, shorted $90^0$ Sectoral MSAs were fabricated using copper plate of finite thickness. The antennas were supported in air using foam spacer support which was placed towards the open circuit edges of the shorted patch. The compact MSA was coaxially fed using N-type connector of 0.32 cm inner wire diameter. The measurement was carried out on finite square ground plane of side length 30 cm using ZVH-8 vector network analyzer.

## 2. SHORTED $90^0$ SECTORAL MSA

The top and side view of coaxially fed CMSA is shown in Fig. 1(a, b). The CMSA is suspended above the ground plane using air substrate of thickness ‘h’. The field distribution at the fundamental $TM_{11}$ mode in CMSA is also shown in Fig. 1(a). The resonance frequency of CMSA for the given patch radius is calculated by using equation (1) [1 – 4].

$$f_{TMmn} = \frac{k_{mn} c}{2 a_e \sqrt{\varepsilon_r}} \quad (1)$$

The ‘$a_e$’ is the effective patch radius which accounts for extension in patch radius due to the fringing fields. The equation for extension in radius due to fringing fields is available for thinner substrates. The $k_{mn}$ indicates the $n^{th}$ root of $m^{th}$ order Bessel function of second type and it is equal to 1.84118 for $TM_{11}$ mode. The shorted semi-circular MSA is derived by placing the shorting post along the zero field line of $TM_{11}$ mode and by using half of the patch size as shown in Fig. 1(c). The shorted semi-circular MSA on thinner substrate has nearly the same resonance frequency and BW to that given by circular MSA. The shorted $90^0$ Sectoral MSA is derived by using the symmetry of shorted semi-circular MSA across the feed point axis and by using half of the shorted MSA as shown in Fig. 1(d). The shorted $90^0$ Sectoral MSA yields nearly 75% reduction in patch size as compared to CMSA. To design shorted $90^0$ Sectoral MSA, resonance frequency formulation for CMSA on thinner substrate gives closer result. However design steps/formulations to calculate the shorted $90^0$ Sectoral patch radius for thicker substrate ($h>0.04\lambda_0$) over wide range of frequencies is not available. Therefore designing of compact shorted $90^0$ Sectoral patch relies upon the parametric optimization of patch radius using simulation software. Therefore to realize accurate prediction of shorted patch radius in shorted $90^0$ Sectoral MSA and its edge extension length in terms of substrate thickness, an ANN model for shorted $90^0$ Sectoral MSA is developed as discussed below.

## 3. ANN MODEL FOR SHORTED $90^0$ SECTORAL MSA

The ANN model for shorted $90^0$ Sectoral MSA is developed for substrate thickness increasing from 0.04 to $0.1\lambda_0$ and for the frequency range from 800 to 6000 MHz. Since in most of the reported compact MSAs, an air substrate is used (since it helps in realizing maximum radiating efficiency), the same is selected here for developing the ANN model.

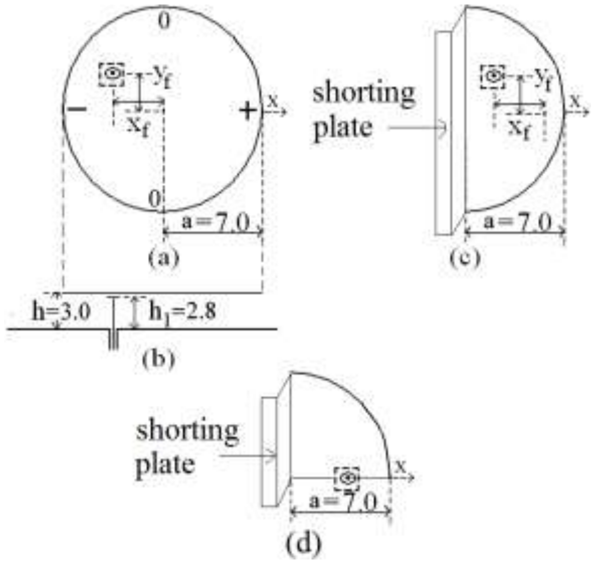


**Fig 1: (a) Top and (b) views of proximity CMSA, (c) proximity fed shorted semi-circular MSA and (d) proximity fed shorted $90^0$ Sectoral MSA**

At given frequency and increasing substrate thickness, to develop an ANN model, training data sets is generated using IE3D software. At the given frequency, for substrate thickness ‘h’, the shorted $90^0$ Sectoral MSA length is taken equal to quarter wave in length ($r_e$). The shorted $90^0$ Sectoral patch is simulated using IE3D software and peak in the resonance curve is noted. If the peak does not coincide with the desired frequency, shorted Sectoral patch radius is altered and the shorted patch is simulated again. This procedure is repeated un-till the peak in the resonance curve coincides with the desired shorted $TM_{11}$ mode resonance frequency. For this frequency matching, simulated shorted patch radius ‘r’ is noted and fringing field extension length is calculated by using the following equation.

$$\Delta r = \lambda/4 - r \quad (2)$$

At a given frequency for six to eight substrate thickness values, data set of shorted patch radius and fringing field extension length is calculated. This procedure is repeated over wide frequency range and at different substrate thickness. The training date set are generated such that at each frequency ‘h’ is less than or equal to $0.1\lambda_0$. The above procedure for generation of training data sets is shown in Fig. 2. The data sets were generated at every 100 MHz frequency intervals over 800 to 6000 MHz frequency band. At each frequency parameters like, edge extension length in terms of substrate thickness, shorted patch radius, frequency and dielectric constant of substrate (air in this case) are used to develop an ANN model. The feed-forward standard back-propagation algorithm is used as a neural network model for shorted $90^0$ Sectoral MSA. This is a supervised neural network model. The neural network model for shorted $90^0$ Sectoral MSA is shown in Fig. 3(a, b).

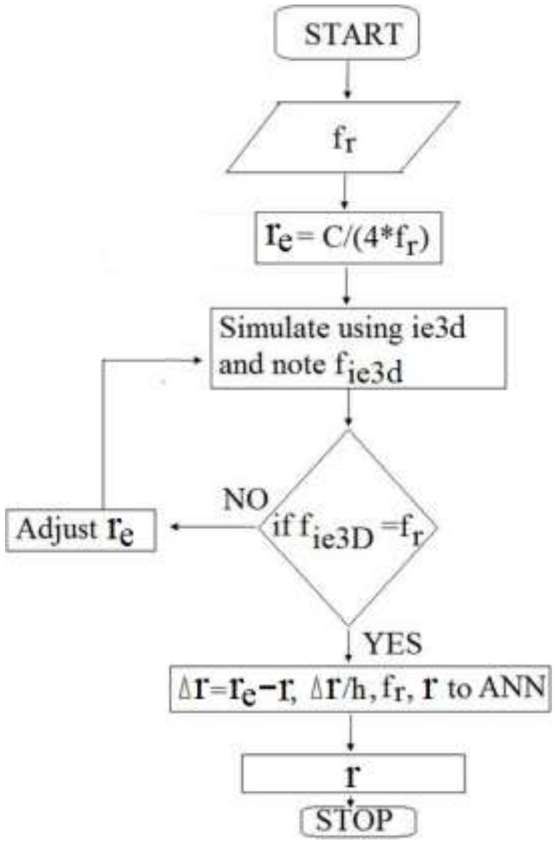


**Fig 2: Flowchart for calculating shorted $90^0$ Sectoral MSA radius**

The supervised network is trained using input data and target data. The neural network learns from the input data and transforms input data into a desired response with the help of target data. They can approximate virtually any input-output map. They have been shown to approximate the performance of optimal statistical classifiers in difficult problems. The basic MLP (multi-level perceptron) building unit is a simple model of artificial neurons. This unit computes the weighted sum of the inputs plus the threshold weight and passes this sum through the activation function. In a multi-layer perceptron, the outputs of the units in one layer forms the inputs to the next layer. The weights of the network are usually computed by training the network using the back propagation algorithm. The supervised network, which has a configuration of 4 input neurons, 10 hidden neurons in a hidden layer and 2 output neurons which is trained for 50 epochs. The ANN model is trained with 6 samples and tested with the samples which fall under $0.1\lambda_0$ samples determined according to the definition of the problem. The parameters fed to the input of ANN are substrate thickness, fringing field extension length, dielectric constant at different resonant frequencies. The shorted patch radius at different shorted $TM_{11}$ mode resonant frequencies and for different substrate thickness is predicted at the output of a trained neural network. For the predicted value, shorted $90^0$ Sectoral MSA is simulated using IE3D software and the resonance frequency is observed from its resonance curve plot. The % error between the simulated and actual desired value (as given by ANN model) is calculated. The results obtained using ANN model for different frequencies and substrate thickness are tabulated in Table 1 to 17. They show close matching with simulated frequencies.

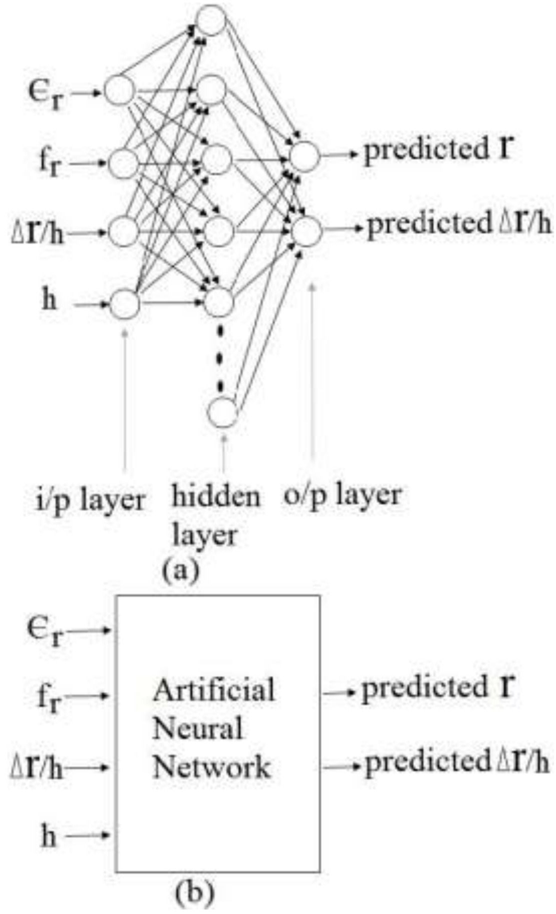


**Fig 3: (a, b) ANN model for shorted $90^0$ Sectoral MSA**

To validate the ANN and simulated results, measurements were carried out. At each frequency points shorted patch is fabricated using copper plate of finite thickness. The shorted patch is suspended in air using foam spacer support placed towards the antenna corners. The measurement was carried out using R & S VNA (ZVH 8). The measured values are also in close agreement with predicted and simulated results as given in respective tables. Thus proposed ANN model can be used to accurately calculate the shorted patch radius and edge extension length in terms of substrate thickness at any desired frequency and substrate thickness.

**Table 1. Comparison between simulated, predicted and measured results at 1200 MHz**

| h (cm) | $h/\lambda_o$ | $f_{ie3d}$ (MHz) | $f_{ANN}$ (MHz) | $f_{measured}$ (MHz) | % Error |
|---|---|---|---|---|---|
| 1 | 0.04 | 1228 | 1200 | 1242 | 2.33 |
| 1.2 | 0.048 | 1194 | 1200 | 1236 | 0.5 |
| 1.5 | 0.06 | 1219 | 1200 | 1196 | 1.58 |
| 1.8 | 0.072 | 1189 | 1200 | 1160 | 0.92 |
| 2.0 | 0.08 | 1187 | 1200 | 1221 | 1.1 |
| 2.4 | 0.096 | 1168 | 1200 | 1180 | 2.67 |

**Table 2. Comparison between simulated, predicted and measured results at 1700 MHz**

| h (cm) | $h/\lambda_o$ | $f_{ie3d}$ (MHz) | $f_{ANN}$ (MHz) | $f_{measured}$ (MHz) | % Error |
|---|---|---|---|---|---|
| 0.4 | 0.022 | 1784 | 1700 | 1698 | 4.94 |
| 0.6 | 0.033 | 1760 | 1700 | 1732 | 3.53 |
| 0.8 | 0.044 | 1740 | 1700 | 1710 | 2.35 |
| 1.0 | 0.055 | 1754 | 1700 | 1685 | 3.17 |
| 1.4 | 0.077 | 1686 | 1700 | 1745 | 0.823 |
| 1.6 | 0.088 | 1646 | 1700 | 1675 | 3.17 |

**Table 3. Comparison between simulated, predicted and measured results at 1800 MHz**

| h (cm) | $h/\lambda_o$ | $f_{ie3d}$ (MHz) | $f_{ANN}$ (MHz) | $f_{measured}$ (MHz) | % Error |
|---|---|---|---|---|---|
| 0.6 | 0.035 | 1814 | 1800 | 1785 | 0.78 |
| 0.8 | 0.047 | 1772 | 1800 | 1832 | 1.56 |
| 1.2 | 0.071 | 1868 | 1800 | 1779 | 3.78 |
| 1.4 | 0.082 | 1818 | 1800 | 1776 | 1 |
| 1.6 | 0.094 | 1796 | 1800 | 1820 | 0.22 |

**Table 4. Comparison between simulated, predicted and measured results at 1900 MHz**

| h (cm) | $h/\lambda_o$ | $f_{ie3d}$ (MHz) | $f_{ANN}$ (MHz) | $f_{measured}$ (MHz) | % Error |
|---|---|---|---|---|---|
| 0.6 | 0.037 | 1966 | 1900 | 1905 | 3.47 |
| 0.8 | 0.050 | 1900 | 1900 | 1922 | 0 |
| 1.1 | 0.068 | 1812 | 1900 | 1915 | 4.63 |
| 1.3 | 0.081 | 1815 | 1900 | 1865 | 4.47 |

**Table 5. Comparison between simulated, predicted and measured results at 2000 MHz**

| h (cm) | $h/\lambda_o$ | $f_{ie3d}$ (MHz) | $f_{ANN}$ (MHz) | $f_{measured}$ (MHz) | % Error |
|---|---|---|---|---|---|
| 1.0 | 0.067 | 1920 | 2000 | 1986 | 4 |
| 1.1 | 0.073 | 2084 | 2000 | 2010 | 4.2 |
| 1.2 | 0.080 | 2024 | 2000 | 2032 | 1.2 |
| 1.3 | 0.087 | 2002 | 2000 | 1977 | 0.1 |
| 1.4 | 0093 | 2000 | 2000 | 2004 | 0 |

**Table 6. Comparison between simulated, predicted and measured results at 1700 MHz**

| h (cm) | $h/\lambda_o$ | $f_{ie3d}$ (MHz) | $f_{ANN}$ (MHz) | $f_{measured}$ (MHz) | % Error |
|---|---|---|---|---|---|
| 0.8 | 0.056 | 2009 | 2100 | 2100 | 4.33 |
| 0.9 | 0.063 | 2188 | 2100 | 2067 | 4.19 |
| 1.1 | 0.077 | 2095 | 2100 | 2120 | 0.23 |
| 1.2 | 0.084 | 2065 | 2100 | 2102 | 1.67 |
| 1.4 | 0.098 | 2102 | 2100 | 2094 | 0.048 |

**Table 7. Comparison between simulated, predicted and measured results at 2500 MHz**

| h (cm) | $h/\lambda_o$ | $f_{ie3d}$ (MHz) | $f_{ANN}$ (MHz) | $f_{measured}$ (MHz) | % Error |
|---|---|---|---|---|---|
| 0.5 | 0.042 | 2484 | 2500 | 2496 | 0.64 |
| 0.6 | 0.05 | 2502 | 2500 | 2518 | 0.008 |
| 0.7 | 0.058 | 2484 | 2500 | 2478 | 0.64 |
| 0.8 | 0.067 | 2436 | 2500 | 2510 | 2.56 |
| 1.0 | 0.0833 | 2372 | 2500 | 2485 | 5.12 |

**Table 8. Comparison between simulated, predicted and measured results at 2700 MHz**

| h (cm) | $h/\lambda_o$ | $f_{ie3d}$ (MHz) | $f_{ANN}$ (MHz) | $f_{measured}$ (MHz) | % Error |
|---|---|---|---|---|---|
| 0.3 | 0.027 | 2748 | 2700 | 2695 | 1.78 |
| 0.4 | 0.064 | 2628 | 2700 | 2710 | 2.67 |
| 0.9 | 0.082 | 2784 | 2700 | 2705 | 3.11 |
| 1.0 | 0.091 | 2828 | 2700 | 2688 | 4.74 |

**Table 9. Comparison between simulated, predicted and measured results at 3000 MHz**

| h (cm) | $h/\lambda_o$ | $f_{ie3d}$ (MHz) | $f_{ANN}$ (MHz) | $f_{measured}$ (MHz) | % Error |
|---|---|---|---|---|---|
| 0.3 | 0.030 | 3008 | 3000 | 3012 | 2.67 |
| 0.4 | 0.04 | 3004 | 3000 | 2986 | 0.13 |
| 0.5 | 0.05 | 3132 | 3000 | 3120 | 4.4 |
| 0.6 | 0.06 | 3096 | 3000 | 3002 | 3.2 |
| 0.7 | 0.07 | 3036 | 3000 | 3018 | 1.2 |

**Table 10. Comparison between simulated, predicted and measured results at 3500 MHz**

| h (cm) | $h/\lambda_o$ | $f_{ie3d}$ (MHz) | $f_{ANN}$ (MHz) | $f_{measured}$ (MHz) | % Error |
|---|---|---|---|---|---|
| 0.4 | 0.046 | 3596 | 3500 | 3498 | 2.74 |
| 0.45 | 0.052 | 3588 | 3500 | 3512 | 2.51 |
| 0.5 | 0.058 | 3508 | 3500 | 3526 | 0.23 |
| 0.55 | 0.064 | 3500 | 3500 | 3489 | 0 |

**Table 11. Comparison between simulated, predicted and measured results at 3700 MHz**

| h (cm) | $h/\lambda_o$ | $f_{ie3d}$ (MHz) | $f_{ANN}$ (MHz) | $f_{measured}$ (MHz) | % Error |
|---|---|---|---|---|---|
| 0.5 | 0.061 | 3680 | 3700 | 3696 | 0.54 |
| 0.6 | 0.074 | 3700 | 3700 | 3688 | 0 |
| 0.7 | 0.086 | 3700 | 3700 | 3712 | 0 |
| 0.75 | 0.093 | 3700 | 3700 | 3686 | 0 |
| 0.8 | 0.099 | 3642 | 3700 | 3721 | 1.57 |

**Table 12. Comparison between simulated, predicted and measured results at 4000 MHz**

| h (cm) | $h/\lambda_o$ | $f_{ie3d}$ (MHz) | $f_{ANN}$ (MHz) | $f_{measured}$ (MHz) | % Error |
|---|---|---|---|---|---|
| 0.35 | 0.047 | 3920 | 4000 | 3995 | 2 |
| 0.4 | 0.053 | 4013 | 4000 | 4041 | 0.33 |
| 0.45 | 0.060 | 3855 | 4000 | 4025 | 3.63 |
| 0.5 | 0.067 | 3984 | 4000 | 4010 | 0.4 |
| 0.6 | 0.080 | 4118 | 4000 | 4022 | 2.95 |

**Table 13. Comparison between simulated, predicted and measured results at 4200 MHz**

| h (cm) | $h/\lambda_o$ | $f_{ie3d}$ (MHz) | $f_{ANN}$ (MHz) | $f_{measured}$ (MHz) | % Error |
|---|---|---|---|---|---|
| 0.4 | 0.056 | 4240 | 4200 | 4195 | 0.95 |
| 0.45 | 0.063 | 4168 | 4200 | 4176 | 0.76 |
| 0.55 | 0.704 | 4200 | 4200 | 4211 | 0 |
| 0.6 | 0.085 | 4186 | 4200 | 4206 | 0.33 |

**Table 14. Comparison between simulated, predicted and measured results at 4500 MHz**

| h (cm) | $h/\lambda_o$ | $f_{ie3d}$ (MHz) | $f_{ANN}$ (MHz) | $f_{measured}$ (MHz) | % Error |
|---|---|---|---|---|---|
| 0.4 | 0.059 | 4462 | 4500 | 4486 | 0.84 |
| 0.45 | 0.067 | 4406 | 4500 | 4492 | 2.09 |
| 0.55 | 0.082 | 4678 | 4500 | 4510 | 3.96 |
| 0.6 | 0.089 | 4642 | 4500 | 4487 | 3.16 |

**Table 15. Comparison between simulated, predicted and measured results at 4800 MHz**

| h (cm) | $h/\lambda_o$ | $f_{ie3d}$ (MHz) | $f_{ANN}$ (MHz) | $f_{measured}$ (MHz) | % Error |
|---|---|---|---|---|---|
| 0.25 | 0.040 | 4780 | 4800 | 4756 | 0.42 |
| 0.3 | 0.048 | 4684 | 4800 | 4812 | 2.42 |
| 0.35 | 0.056 | 4918 | 4800 | 4796 | 2.46 |
| 0.5 | 0.080 | 4762 | 4800 | 4789 | 0.79 |

**Table 16. Comparison between simulated, predicted and measured results at 5500 MHz**

| h (cm) | $h/\lambda_o$ | $f_{ie3d}$ (MHz) | $f_{ANN}$ (MHz) | $f_{measured}$ (MHz) | % Error |
|---|---|---|---|---|---|
| 0.25 | 0.045 | 5524 | 5500 | 5514 | 0.44 |
| 0.3 | 0.055 | 5596 | 5500 | 5498 | 1.75 |
| 0.35 | 0.064 | 5796 | 5500 | 5523 | 5.38 |

**Table 17. Comparison between simulated, predicted and measured results at 6000 MHz**

| h (cm) | $h/\lambda_o$ | $f_{ie3d}$ (MHz) | $f_{ANN}$ (MHz) | $f_{measured}$ (MHz) | % Error |
|---|---|---|---|---|---|
| 0.2 | 0.04 | 6106 | 6000 | 6102 | 1.77 |
| 0.35 | 0.07 | 5974 | 6000 | 5986 | 0.43 |
| 0.4 | 0.08 | 6772 | 6000 | 6005 | 2.87 |

# 4. CONCLUSIONS

The ANN model for shorted $90^0$ Sectoral MSA over a wide frequency range and substrate thickness increasing from 0.04 to $0.1\lambda_0$, is proposed. The neural network model is developed using antenna parameters like, substrate thickness, dielectric constant (air), resonance frequency and an edge extension length in terms of substrate thickness. The training data sets spaced at every 100 MHz frequency intervals were used to develop ANN model. The predicted shorted patch radius as obtained from the neural network model which when simulated using IE3D software gives closer match with the desired patch resonance frequency, over increasing substrate thickness. To validate the simulated and predicted frequency results, measurements were carried out. The measured results show closer agreement with predicted and simulated frequencies. As in the world of miniaturization, compact shorted MSAs are frequently needed in various applications. In many applications shorted compact variations of CMSA, i.e. shorted $90^0$ Sectoral MSA finds the application. As the close form expressions to calculate shorted patch radius is not available, the proposed ANN model can be used to design shorted $90^0$ Sectoral MSA on thicker substrate and at any given frequency. In the future work, similar neural network model will be developed to predict the length of shorted MSAs on suspended dielectric substrates.

# 5. REFERENCES

[1] B. Bhartia and I. J. Bahl, Microstrip Antennas, USA, 1980.

[2] Kumar, G., Ray, K. P., 2003. Broadband Microstrip Antennas, 1st edn., Artech House, USA.

[3] Wong, K. L., 2002. Compact and Broadband Microstrip Antennas, 1st edn., John Wiley & sons, Inc., New York, USA.

[4] Garg, R., Bhartia, P., Bahl, I., Ittipiboon, A., 2001. Microstrip Antenna Design Handbook, Artech House, USA.

[5] Kushwah, V. S., Tomar, G. S., 2009. Design of Microstrip Patch Antennas Using Neural Network, Proceedings of Third Asia International Conference on Modelling & Simulation, Bali, (DOI - 10.1109/AMS.2009.12).

[6] Turker, N., Gunes, F., Yildirim, T., 2006. Artificial Neural Design of Microstrip Antennas, Turk J Elec Engin, 14, 3, 445 – 453.

[7] Can, S., Kapusuz, K. Y., and Aydin, E., Calculation of Resonant frequencies of a shorting pin-loaded ETMSA with ANN, Microwave and Optical Technology Letters, Vol. 56, No. 3, March 2014, 660 – 663.

[8] Kapusuz, K. Y. Tora, H., and Can, S., Neural network based estimation of resonant frequency of an equilateral triangular microstrip antenna, Tech Gaz, 20, 2013, 1 – 6.

[9] Sagiroglu, S., and Guney, K., Calculation of Resonant frequency for an equilateral triangular microstrip antenna with the use of artificial neural networks, Microwave and Optical Technology Letters, Vol. 14, 1997, 89 – 93.

[10] Deshmukh, Amit A., Kulkarni, Shivali D., Venkata, A. P. C., and Phatak, Neelam V., Artificial Neural Network Model for Suspended Rectangular Microstrip Antennas, Proceedings of ICAC3 – 2015, 1st & 2nd April 2014, Mumbai, India

[11] Deshmukh, Amit A., Kulkarni, Shivali D., Venkata, A. P. C., and Phatak, Neelam V., Artificial Neural Network Model for Suspended Rectangular Microstrip Antennas, Proceedings of ICAC3 – 2015, 1st & 2nd April 2014, Mumbai, India

[12] IE3D 12.1, Zeland Software, Freemont, USA, 2004.